

Progress in polar upper atmospheric physics research in China

LIU Ruiyuan* & YANG Huigen

Polar Research Institute of China, Shanghai 200136, China

Received 3 April 2012; accepted 25 May 2012

Abstract The Chinese Antarctic Great Wall, Zhongshan, Kunlun and Arctic Yellow River stations have unique geographical locations, well suited to carry out polar upper atmospheric observations. This paper reviews the tremendous history of nearly 30 years of Chinese polar expeditions and major progress in polar upper atmospheric physics research. This includes the polar upper atmospheric physics conjugate observation system at Zhongshan Station in the Antarctic and Yellow River Station in the Arctic, and original research achievements in polar ionospheric fields, aurora and particle precipitation, the polar current system, polar plasma convection, geomagnetic pulsations and space plasma waves, inter-hemispheric comparisons of the space environment, space weather in polar regions, power spectrum of the incoherent scatter radar, ionospheric heating experiments and polar mesospheric summer echoes, polar ionosphere-magnetosphere numerical simulation and others. Finally, prospects for Chinese polar upper atmospheric physics research are outlined.

Keywords upper atmospheric physics, space physics, geospace, polar region, ionosphere, aurora

Citation: Liu R Y, Yang H G. Progress in polar upper atmospheric physics research in China. *Adv Polar Sci*, 2012, 23: 55-71, doi: 10.3724/SP.J.1085.2012.00055

0 Introduction

The polar upper atmosphere is an important part of the geospace system on which human survival and development depends. The geospace environment is vulnerable to solar storms and produces disastrous space weather, which can seriously threaten space flights, communication, navigation, power grids, astronaut health, space security and others. Therefore, monitoring, investigating and forecasting the geospace environment are very important.

In geospace research, observations and studies of the polar upper atmosphere occupy an important position. Polar regions are the earth's windows to outer space, where geomagnetic fields enter or exit nearly vertically. Energetic particles from the solar wind enter the Earth's magnetosphere and then precipitate into the polar ionosphere and upper and middle atmosphere along magnetic field lines. This results in a series of important geophysical phenomena, such as auroras, magnetic storms, substorms, ionospheric

storms, polar cap absorption, western surge, heating and ionization of the middle atmosphere, among others. These space weather processes occur earliest and strongest in polar regions, and gradually propagate to mid and low latitudes. The polar upper atmosphere is one of the most active parts of Earth's atmosphere. It has strong coupling to the middle and low atmosphere, and sensitive response and clear feedback to global changes. Therefore, study of the upper polar atmosphere facilitates greater understanding of the nature of solar wind-magnetosphere-ionosphere-upper/middle atmosphere interactions and global changes.

Chinese polar research has spanned nearly 30 years, since the first Antarctic expedition in 1984. Vigorous development of such expeditions has created a new research area in upper polar atmospheric physics. China has the most ancient aurora records in the world, but had no systematic auroral observation because of geographic constraints. Establishment of the Chinese Antarctic Great Wall, Zhongshan and Kunlun stations, and the Arctic Yellow River Station, has provided observation bases for upper polar atmospheric research. We have achieved remarkable progress in this field after 30 years of effort. In this paper, we briefly

* Corresponding author (email: ryliu@pric.gov.cn)

introduce the observation systems, review major achievements, and outline future prospects in the study of upper polar atmospheric physics in China. The measurement system description is based on current operations, and the research progress is focused on recent years. Earlier activities can be found in references^[1-4].

1 Chinese upper atmosphere physics observation systems in polar regions

The Chinese Antarctic Great Wall, Zhongshan, and Kunlun stations, and the Arctic Yellow River Station, all have unique geographic locations for geospace environment

monitoring and are very suitable for polar upper atmosphere physics (UAP) observation and study. Establishment months and geographic and corrected geomagnetic (CGM) coordinates of these stations are listed in Table 1. Chinese UAP observation systems are listed in Table 2.

The Antarctic Great Wall Station is located in the sub-aurora zone, Weddell Sea ionospheric anomaly and South Atlantic magnetic anomaly zone. It is in a special area for the geospace environment and is a unique space environment monitoring station for China in the Western Hemisphere. Ionospheric and geomagnetic observations have been made for solar-terrestrial space research at this station.

Table 1 Geographic and corrected geomagnetic coordinates of Great Wall, Zhongshan, Kunlun stations in Antarctica, and Yellow River Station in the Arctic

Station	Setup time (MM/YYYY)	Geographic Coordinates		CGM Coordinates (2005)	
		Latitude	Longitude	Latitude	Longitude
Great Wall	02/1985	62°12'59"S	58°57'52"W	-47.75°	11.48°
Zhongshan	02/1989	69°22'24"S	76°22'40"E	-74.63°	96.66°
Kunlun	02/2009	80°25'01"S	77°06'58"E	-77.92°	54.32°
Yellow River	07/2004	78°55'12"N	11°55'48"E	76.30°	110.52°

Table 2 Observing instruments for polar upper atmospheric physics at Chinese polar stations

Station	Instrument	Measured parameters	Mode	Start time—end time
Great Wall	Digisonde	Ionogram and routine ionospheric characteristics	Automatic observation + manual correction	1987—2000
	GPS scintillation	Scintillation index, TEC	Automatic	1999—2007
	Short-wave field strength meter	Field strength	Automatic	1988—present
	ALPHA VLF receiver	Field strength, phase	Automatic	1987—2000
Zhongshan	Digisonde	Ionogram and drift velocity	Routine operation, 8 times per hour	1995—present
	All-sky TV camera	Aurora intensity in all-sky	Operates in time, analogue video signal or digitized sampling rate at 4 s	1995—present
	Meridian scanning photometer	Absolute aurora intensities of the wavelengths 427.8 nm, 557.7 nm and 630.0 nm along the magnetic N-S meridian line	Operation during dark time, sampling rate at 8 s	1995—present
	Induction magnetometer	Variation rates of geomantic H and D components	Routine operation, sampling rate at 0.5—2 s	1995—present
	Fluxgate magnetometer	Relative variations of geomagnetic X, Y and Z components	Routine operation, sampling rate at 1 s	1995—2006
	Imaging riometer	2D ionosphere absorption of the cosmic noise	Routine operation, sampling rate at 4 s	1998—present
	CCD monochromatic all-sky camera	Aurora intensities of wavelength 557.7 nm/630 nm in all-sky	Operation during dark time, exposure time: 10 s, time resolution: 15 s	1998—present
	Zhongshan-Kunlun low power magnetometer chain	Relative variations of geomagnetic X, Y and Z components	Routine operation, sampling rate at 1 s	2007—present

(To be continued on the next page)

(Continued)

Zhongshan	G856 Proton magnetometer	Geomagnetic total intensity	Twice a week	1989—present
	CTM-DI magnetometer	Geomagnetic D and I components	Twice a week	1989—present
	Digital magnetic variation instrument	Relative variations of geomagnetic D, H and Z components	Routine operation	1989—present
	CMJ92 and ULFO2 pulse analyzer	Geomagnetic pulsation	Routine operation	1989—present
	VLF receiver	Whistle	Synchronizes with all-sky TV camera	1989—present
	HF coherent scattering radar	Ionospheric convection speed, spectral broadening and echo intensity	Routine operation, time resolution in 3 min	2010—present
	Aurora spectrograph	Aurora spectrum intensity along the magnetic N-S meridian line	Operation during dark time, sample rate at 10 s	2010—present
	Multiple wavelengths aurora CCD imager system	2D aurora intensities of wavelength 427.8 nm, 557.7 nm and 630 nm	Operation during dark time, sample rate less than 10 s	2010—present
	GPS scintillation network	TEC, scintillation index, ionospheric drift	Routine operation	2010—present
Yellow River	3 wavelengths aurora CCD imager system	2D aurora intensities of wavelength 427.8 nm, 557.7 nm and 630 nm	Operation during dark time, sample rate less than 10 s	2003—present
	Imaging riometer	2D ionosphere absorption of the cosmic noise	Automatic, sampling rate 4 s	1991—present
	GPS scintillation network	TEC, scintillation index, ionospheric drift	Automatic	2006—present

Zhongshan Station, at an invariant geomagnetic latitude of 75 degrees, is under the cusp region at noon and polar cap at night. It passes through the aurora zone twice per day, and numerous ionospheric signatures and aurora phenomena associated with solar-terrestrial energy transportation can be observed there. Zhongshan Station is a unique place for geospace environment monitoring and is among very few polar stations for post-noon aurora observation. After scientific collaboration between China and Japan in the ninth five-year plan, construction during the polar research expedition in the tenth five-year plan, and the international polar year (IPY) in the eleventh five-year plan, a first-rank space environment monitoring system was built at Zhongshan Station that makes optic, geomagnetic and radio observations. Site instrumentation consists of a digisonde, all-sky TV camera, meridian-scanning photometer, induction magnetometer, fluxgate magnetometer, imaging riometer, CCD monochromatic all-sky camera, and low power magnetometer chain between Zhongshan and Kunlun stations. An HF coherent scattering radar, aurora spectrograph, set of aurora multiple wavelength imagers, and GPS scintillation network were installed in 2010.

Kunlun Station is inland, atop Dome A in the Antarctic. It is also under the cusp region and combined with Zhongshan Station, extends spatiotemporal upper atmospheric observation of the cusp region.

The Arctic Yellow River Station is at Ny-Ålesund in

the Svalbard archipelago. It is under the cusp region in the Northern Hemisphere, and geomagnetic conjugate with Zhongshan Station in Antarctica. The polar night at Yellow River Station lasts about four months, which means that the station is ideal for aurora and other upper atmosphere observations, and for high-latitude conjugacy studies. In November 2003, a set of three-wavelength aurora CCD all-sky imager (ASI) systems was installed at Yellow River Station. Thus began continuous and simultaneous observations of three-wavelength (427.8 nm, 557.7 nm and 630 nm) aurora emission intensities and two-dimensional particle precipitation, with time resolution less than 10 s. In August 2004 an imaging riometer system set up in 1991 by Nagoya University, Japan was transferred to the Polar Research Institute of China (PRIC). The system was completely upgraded by PRIC in October 2008, achieving real-time monitoring. For ionospheric irregularity and associated signal scintillation studies, a GPS scintillation measurement system was installed in 2006, and upgraded to a triangle monitoring network in 2007 for irregularity drift measurement. There are rich and advanced international space environment observation facilities around Yellow River Station, such as the European Incoherent Scatter (EISCAT) Radar, Super Dual Auroral Radar Network (SuperDARN), international SPEAR ionosphere heating system, and the Norwegian Andøya rocket range. This shows that Yellow River Station is an ideal site for the international space environment ob-

servational campaign.

The instruments at Zhongshan and Yellow River stations comprise an advanced polar upper atmosphere physics conjugate observation system at cusp region latitudes. There has been routine observation at these stations since instrument installation. Average annual recorded data for routine operational instruments is about 150 GB. Optic aurora data is from about 1 000 h at Zhongshan Station, and 1 700 h (900 GB) at Yellow River Station. Polar upper atmosphere physics data has been accumulated for many years, with continuous monitoring of the space environment in the polar region.

Many data analysis platforms have been developed, such as an all-sky TV camera data analysis system, induction magnetometer analysis system. Ionogram interpretation and drift data analysis methods dedicated to digisonde data have been improved. Raw data has been manually interpreted and arranged, and ionospheric and geomagnetic observation datasets have been published. Partial datasets have been published online as the Zhongshan/Yellow River Station aurora database (<http://aurora.chinare.org.cn>), Zhongshan Station digisonde database (<http://dps4.chinare.org.cn>), and Zhongshan Station geomagnetic database (<http://geomag.chinare.org.cn>).

2 Progress in polar upper atmospheric physics research in China

Since the first Chinese Antarctic Scientific Expedition in 1984, polar upper atmospheric physics has been one of the most important subjects of polar research. Several national research programs have been continuously dedicated to this subject. More than 10 groups have been involved in this research field, within the Chinese Academy of Sciences, Ministry of Education, Ministry of Information Industry, China Meteorological Administration, State Seismological Bureau, and State Oceanic Administration. A high quality research team has been formed, with young and middle-aged members. This team has made achievements in research of the polar ionosphere, aurora and magnetosphere, upper atmosphere and others, receiving international peer attention.

International cooperation and academic exchanges have played an important role in promotion. The Polar Research Institute of China have signed polar upper atmospheric physics cooperative research agreements with the National Institute of Polar Research, Japan, the University of Newcastle, Australia, and the University of Tromsø and University of Oslo in Norway, respectively. These agreements led to execution of two key projects of the Department of Science and Technology, “Inter-hemispheric comparisons of the space environment in the polar region” and “Cooperation of cusp aurora observation and research at Chinese Arctic Yellow River Station”, and to the successful organization of five bilateral colloquiums on polar upper atmospheric physics, with Japan, Norway, and Britain.

2.1 The polar ionosphere

2.1.1 Polar ionosphere at Great Wall Station

By analyzing observed data from the domestic digisonde at the Great Wall Station, diurnal variation of ionospheric $F2$ layer critical frequency (f_0F2) was found to show the Weddell Sea anomaly. In summer, the peak of f_0F2 appears at night and the minimum during the day. Solar radiation and neutral wind in the thermosphere were considered principal causes for the anomaly^[5-8].

2.1.2 Polar ionosphere at Zhongshan Station

Many authors have discussed variability of f_0F2 at Zhongshan Station^[9-18]. Figure 1 shows statistical results deduced from the Digisonde Portable Sounder-4. There are obvious diurnal and annual variations of f_0F2 at Zhongshan Station. The diurnal variation is dominant compared to semidiurnal variation, and the annual variation is dominant relative to semiannual variation. There is a “magnetic noon anomaly” of the diurnal variation, which may be due to soft electron precipitation and polar plasma convection in the cusp region. Since Zhongshan Station is located at high geographic and geomagnetic latitude, both extreme changes of solar radiation and the driving factor from the magnetosphere should be taken into account. At solar maximum, vibrationally excited nitrogen (N_2) may be important in the semiannual anomaly at Zhongshan Station.

Liu et al.^[19] examined ionospheric absorption in early May 1998, using data from the imaging riometer at Zhongshan Station. The two dimensional velocity of a strong absorption spike at 06:39 UT on 2 May was revealed. There was a typical midnight absorption spike event at 22:22 UT on 2 May. Nishino et al.^[20-22] showed night side and post-noon ionospheric absorption observed by polar cusp/cap conjugate stations (Zhongshan Station and Ny-Ålesund). Yamagishi et al.^[23] studied interhemispheric conjugacy of auroral poleward expansion observed by conjugate imaging riometers, at $\sim 67^\circ$ and 75° — 77° invariant latitude. Deng et al.^[24-25] identified 198 ionospheric absorption spikes in imaging riometer data from 2000 to 2001 at Zhongshan Station. Statistical features were discerned, regarding their occurrence, duration, intensity, shape, size, movement and relationship with K_p . Possible mechanisms causing the spike events were also suggested.

Wan et al.^[26] investigated the polar Sporadic E (E_s) related to the electric field in the ionosphere. They modeled the accumulation process of Fe^+ , by solving the continuity and static momentum equations with a simple atmospheric model. The results suggest that electric fields of different orientations could produce two kinds of E_s .

Meng et al.^[27] analyzed polar ionospheric behavior and characteristics of polar patches during the geomagnetic storm of 6—10 November, 2004, using GPS observations from a perennial GPS station at Zhongshan Station and other IGS stations.

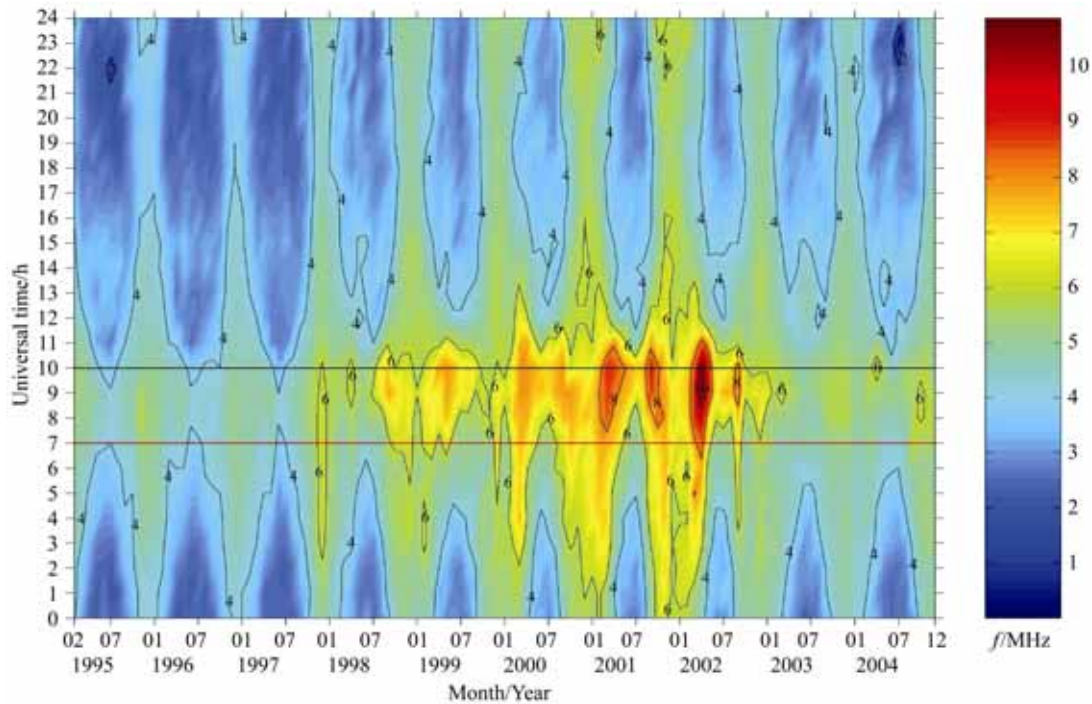


Figure 1 Mean properties of high-latitude ionospheric variation of f_0F_2 at Zhongshan Station.

2.1.3 Polar ionosphere in the Arctic

Using EISCAT (European Incoherent Scatter) radar observations during 1988—1999, climatological features of electron densities in the auroral ionospheric F_2 region have been statistically investigated and compared with the IRI-2001 model, for various seasons and phases of the solar cycle. Average 2-D distributions of EISCAT Ne versus UT and height H, as well as diurnal TEC variations up to 500 km, are reasonably consistent with those predicted by the IRI-2001 model as a whole. However, electron density above the F_2 peak is too large in the IRI-2001, causing the TEC to be higher than in EISCAT observations^[28]. In comparison with the cusp/polar cap region, the so-called “winter anomaly” does not exist over the ESR site. However, a major maximum of electron density was found before local magnetic midnight in winter. Further, there is always a maximum of electron density around local magnetic noon during daytime, in all three seasons. Compared with IRI-2001, the ESR observations show significant distinctions, especially in the topside ionosphere above 500 km altitude and the winter season^[29].

Zhang et al.^[30] analyzed the polar cap patch, using simultaneous observation of the EISCAT, Tromsø VHF radar, and SuperDARN CUTLASS Finland radar. They concluded that dayside magnetic reconnection may be the main mechanism for the patch, and that its formation is strongly dependent on the dawn-dusk component of the interplanetary magnetic field (IMF).

2.2 Aurora and particle precipitation

China is situated at the middle and low latitudes. The aurora

can only be observed in the far north of the country, when geomagnetic activity is strong. Therefore, modern aurora observation and research began relatively late. Although some Chinese scientists studied auroral theory, research on auroral observations was minimal^[31-37]. Based on auroral observations from Zhongshan Station in Antarctica and Yellow River Station in the Arctic, some scientific results have been attained, as follows.

2.2.1 Statistical study of auroral synoptic observations

Based on optical observation at Zhongshan Station, Hu et al.^[38] found that the peaks of auroral occurrence were in the post-noon (14:00—18:00 MLT) and midnight (22:00—03:00 MLT) sectors. Using ground-based optical measurements^[39-40], Yang et al.^[41] confirmed existence of the “15 MLT hot spot,” which was determined primarily from satellite observations (Figure 2). They found that there were two peaks of auroral occurrence in the post-noon “hot spot”. One was the peak (13:15—13:45 MLT) of dayside coronal aurora, and the other (15:45—16:15 MLT) was of post-noon arcs.

Using multiple-wavelength auroral data from Yellow River Station in the Arctic, Hu et al.^[42-43] obtained the synoptic distribution of dayside aurora intensity. The distribution confirmed the two peak regions of aurora intensity in dayside oval deduced from satellite observations, namely the pre-noon 09:00 MLT “warm spot” and post-noon 15:00 MLT “hot spot” (Figure 3). Wang et al.^[44] proposed a representation of spatial texture for auroral image based on the local binary pattern (LBP). They obtained occurrence distributions of four primary categories of dayside auroras, by

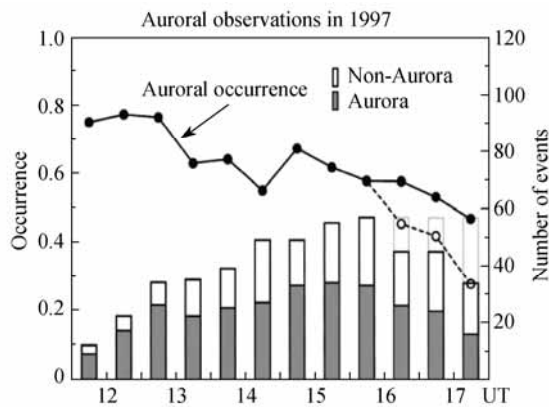


Figure 2 Auroral events and occurrence distributions in post-noon hours at Zhongshan Station.

combining the representation method and automatic image recognition with a supervised classification. Hu et al.^[45] traced magnetospheric sources of dayside auroral active regions along geomagnetic field lines. They asserted that auroral emissions in 09:00/15:00 MLT active regions could be related to pre-noon/post-noon anti-parallel reconnection in the high-latitude magnetopause, and that auroral emissions in 06:30/16:00 MLT active regions are related to Kelvin-Helmholtz instability in the dusk and dawn flank magnetopause. Zhang et al.^[46] found that poleward-moving radar auroral forms (PMAFs) in the 13:00 MLT auroral active region were closely correlated to flux transfer events (FTEs) produced by dayside magnetic reconnection, based on combined observations of the Cluster spacecraft and ASIs at Yellow River Station.

2.2.2 Correlation between aurora and other space environment parameters

Yang et al.^[47] found good correlation between geomagnetic activity and auroral activity at Zhongshan Station. Using binned K_p , Hu et al.^[48-49] found that auroral occurrence (except dayside auroral arcs) and intensity at Zhongshan Station are well correlated with the K_p index. The occurrence rate of strong auroras increases with enhancement of K_p , especially in the post-noon sector. Moreover, the time of crossing the auroral oval for Zhongshan Station is earlier with increasing K_p .

Hu et al.^[50-52] found that post-noon aurora intensity was correlated with the interplanetary magnetic field, and controlled by solar wind electric field and energy. Based on multi-wavelength observation, the 630.0 nm intensity of post-noon aurora shows an increase with enhancement of plasma density, dynamic pressure and velocity of solar wind. The 557.7 nm auroral intensity is not well correlated with the plasma parameters of solar wind. Studying the nightside aurora, Hong et al.^[53-54] discovered that intensity increase of the dusk-midnight-sector auroral arc during a substorm could be produced by lobe reconnection, and rapid intensity decrease was attributed to the IMF B_z turning southward. Moreover, duskward motion of the auroral

arc was controlled by IMF B_y .

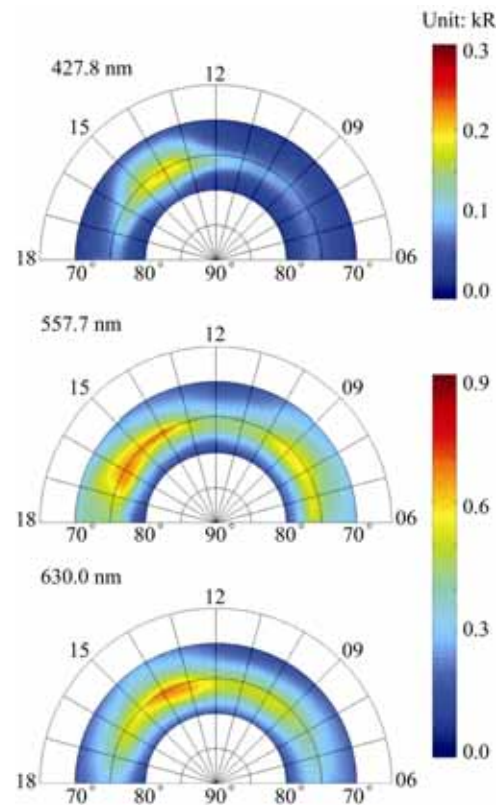


Figure 3 Distribution of average intensity of auroral emissions in MLT-MLAT coordinates, for three wavelengths (427.8, 557.7 and 630.0 nm).

2.2.3 Study of shock aurora

Auroral observations at Zhongshan Station showed that pulsed auroral intensity increased with equatorward drift when dynamic pressure of the solar wind suddenly increased. At the same time, the particle detector on the satellite revealed the inverted-V structure of particle precipitation in the auroral emission region. This could be related to upward and downward field current sheets and field-aligned electron acceleration resulting from field-aligned resonance of the geomagnetic field. This resonance was induced by a negative pulse of dynamic pressure of the solar wind^[55-56].

Using auroral observations from Zhongshan Station /South Pole Station all-sky imagers and ionospheric convection observation from SuperDARN, Liu et al.^[57] showed that auroral intensity increased in the pre-noon sector, but decreased in the post-noon sector when dynamic pressure of the solar wind amplified. At the same time, convection reversion also appeared in the post-noon oval.

2.2.4 Study of auroral particle precipitation

Cai et al.^[58] studied the theory and method of inverting the energy spectrum of auroral precipitating particles, based on electron density profile data from the incoherent scattering radars in the polar region. This is a new way to obtain the

energy spectrum of precipitating particles, and helps improve MLT resolution of energetic particle data from satellites.

Liu et al.^[59] found that different distributions of energy spectra for precipitating particles rarely affects ionospheric conductivity. When energy flux is constant, average energy is the key control on conductivity, and the energy spectra of precipitating particles can markedly change electron density of the *F* layer. When average energy is more than 1 keV, the energy spectrum of particles with modified Maxwell distribution can greatly increase that electron density.

2.3 The current system in polar regions

The field-aligned current is one significant component of the current system in polar regions. Chen et al.^[60] found that region I field-aligned current and its ionospheric current system could not be ignored for its effect on the magnetic field at low latitude. Shen et al.^[61] pointed out that geomagnetic response of the magnetosphere-ionosphere is related to the local time zone of the station, and is caused by the combined effects of the magnetospheric convection and field-aligned currents.

The method of Natural Orthogonal Components (MNO) has been used to study the current system in polar regions. Xu et al.^[62-63] and Sun et al.^[64] studied the equivalent current system in the polar ionosphere, finding that the first eigenvector corresponds to a “directly driven process”, and the second represents the westward electrojet of an “unloading process”. Based on the decomposition described above, some modification can be done on the auroral electrojet (AE) index, which is now widely used to represent the substorm intensity. This obtains related indices associated with magnetospheric convection and the substorm current wedge. The saturation of AE was confirmed by quantitative analysis of it and the polar ionospheric current^[65].

Both auroral display and auroral electrojet, as the most important manifestations of energy coupling between magnetosphere and ionosphere, result from precipitation of particles from the magnetosphere. However, they have different behaviors. Xu et al.^[66] studied dynamic characteristics of the auroral electrojet belt, using equivalent current systems deduced from ground-based magnetic records. Their results showed that the DP2 current system is composed of the eastward electrojet at the dusk side and westward electrojet at the dawn side. These are controlled by the magnetospheric convection electric field, and reflect behavior of the directly driven process. The westward electrojet at the night side is the main component of the DP1 current system, which is controlled by conductivity and reflects the unloading process (Figure 4).

2.4 Polar plasma convections

Liu and Zhu^[67] investigated ionospheric drift obtained with the Digisonde Portable Sounder (DPS-4) at Zhongshan Station in 1995. Statistical analysis revealed main features

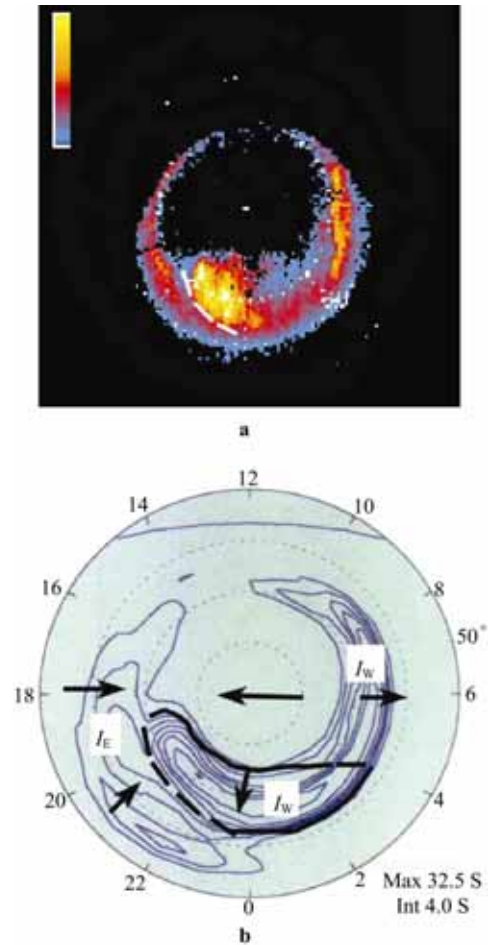


Figure 4 Distribution of auroral intensity (a) and Hall conductance (b) in expanding phase of a substorm. Dashed line in a is Harang zone; arrow in b shows direction of electric field, I_w and I_e are the westward and the eastward electric jet.

of the ionospheric drift. Ionospheric movements at cusp region latitudes are mainly horizontal, and show an average diurnal variation pattern. The ionosphere drifts toward the magnetic South Pole around local noon and away from it at night, coincident with the antisunward convection pattern. Data analysis shows that the convection pattern is largely modulated by the azimuthal component of IMF B_y .

Zhang et al.^[68-70] analyzed the evolution of FTEs generated by dayside reconnections and the effect in the polar ionosphere of both hemispheres. Results revealed near one-to-one correspondence between FTEs observed by spacecraft and PMAFs in the polar ionosphere. Further, ionospheric response time to FTEs in the Northern Hemisphere differs from that in the Southern Hemisphere, which allows inference of locations of the reconnection site (Figure 5).

Hu et al.^[71] studied characteristics of dayside ionospheric convection using northern hemispheric SuperDARN data and DMSP particle and flow observations while the IMF was strongly northward, from 13:00—15:00 UT on 2 March 2002. Results showed a four-cell convection pattern,

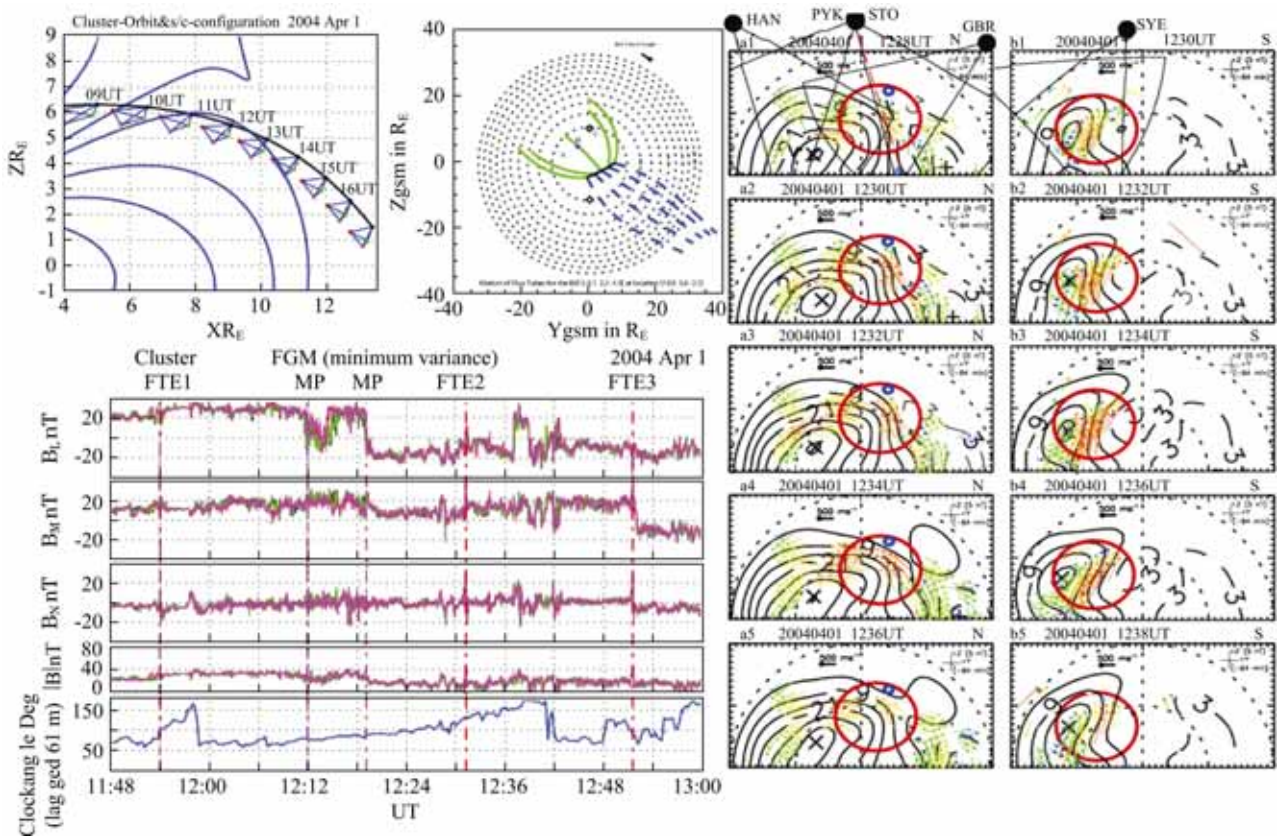


Figure 5 Series of FTEs observed during 11:30–13:00 UT on 1 April 2004, while Cluster spacecraft array was located near high-latitude magnetopause. Directions of velocity enhancements in ionospheric convection of polar regions conjugate observed by SuperDARN radars agree well with Cluster observations and expectations from Cooling analysis.

lasting more than 1.5 h in the Northern Hemisphere. The reconnection rate derived from the SuperDARN data analysis illustrated that high latitude reconnection was quasi-periodic, with period between 4–16 min. A sawtooth-like and reverse-dispersed ion signature was observed by DMSP F14 in the sunward cusp convection around 14:41 UT, confirming that the high latitude reconnection was pulsed. Ac-

companying this pulsed reconnection, strong antisunward ionospheric flow bursts were observed in the post-noon LLBL region on closed field lines, propagating at the same speed as the plasma convection. DMSP flow data show a similar flow pattern and particle precipitation in the conjugate Southern Hemisphere (Figure 6).

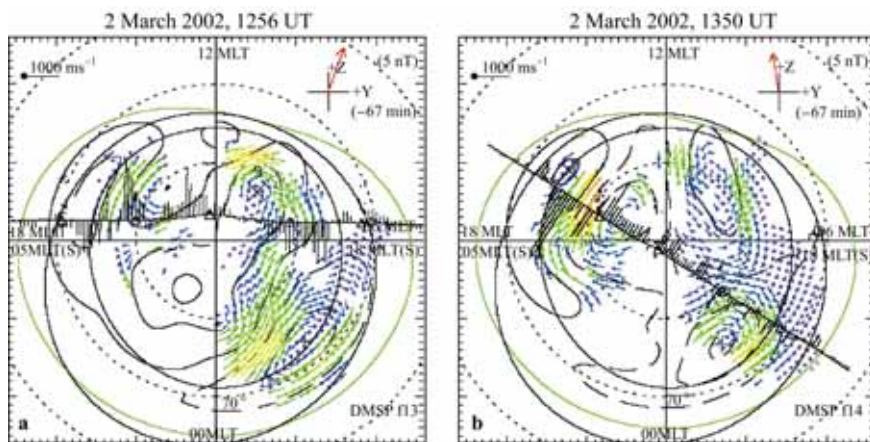


Figure 6 Track and horizontal cross-track velocity data in Southern Hemispheric passages of DMSP F13 during 12:50–13:05 UT (a), and DMSP F14 during 13:43–13:58 UT (b), overlaid on Northern Hemisphere potential map at central time of the passages.

2.5 Geomagnetic pulsations and space plasma waves

Geomagnetic pulsations and space plasma waves have been studied based mainly on conjunction observations between Zhongshan Station and Australia Davis Station, Antarctica. Yang et al.^[72-74] studied occurrence, frequency and amplitude characteristics of Pc3 pulsations observed at Great Wall and Zhongshan stations. Adopting cross spectral analysis techniques, Liu et al.^[75-78] studied Pc3/5 pulsations at cusp latitudes, obtaining their propagation characteristics and local time distribution for amplitude and occurrence. Chief results were: (a) At cusp latitudes, Pc3 pulsations showed obvious daily variation in propagation, occurrence and spectral power. These wave properties also had a certain seasonal variation. (b) The Pc5 pulsations showed a certain daily variation in propagation, occurrence and spectral power. These wave properties also showed a certain seasonal variation. The results indicate that in the daytime, the waves propagated westward at the dawn side and eastward at the dusk side, reversing direction around magnetic local noon. In the nighttime, the Pc5 waves reversed direction around 20:00 MLT, propagating westward before and eastward after this time. Near dusk, Pc5 wave propagation direction was irregular. These characteristics suggest that Pc5 wave sources varied with local time. Yang and Liu^[79] studied polarization characteristics of Pc3 pulsations observed at Zhongshan Station.

Using global geomagnetic field data including those from the polar region, Han et al.^[80] analyzed a typical Pi3 pulsation event, from solar wind perturbations to global response in the magnetosphere. Results suggest that the perturbations may directly drive ULF waves in the magnetosphere (Figure 7).

Liu et al.^[81] obtained Pc3 wave propagation characteristics along magnetic field lines in the exterior cusp region by analyzing waves detected by the four Cluster satellites near the cusp. They found that transverse scale width of the

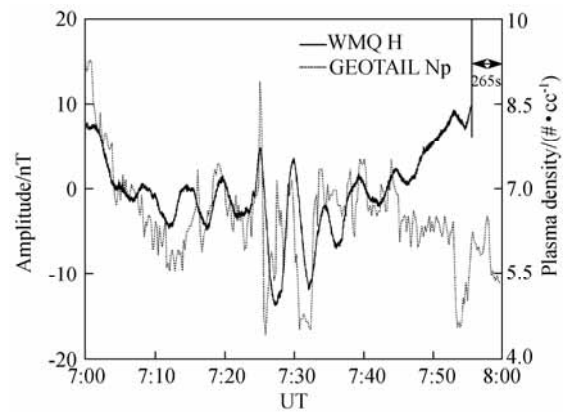


Figure 7 Solar wind dynamic pressure, measured by GEOTAIL spacecraft (dotted line) and H component of magnetic field observed at WMQ (black solid line), on 16 December 2001. Background trend of WMQ data was removed, and time for WMQ was shifted 265 s backward.

Pc3 waves in that region was about 0.14 Re. Shi et al.^[82] analyzed propagation of ULF waves of 0.1–10 Hz from magnetosphere to the ground, considering influences on ground pulsations induced by the ionospheric Alfvén oscillations, magnetic inclination, ionospheric conductivity, and wave frequency.

2.6 Inter-hemispheric comparisons of space environment

Liu et al.^[83] proposed a method of calculating the geomagnetic conjugate point based on conjugate phase of ultra-low frequency (ULF). He obtained the southern polar region conjugate point of Longyearbyen in the Arctic based on geomagnetic data of Pc5 pulsations, and compared it with that calculated by geomagnetic model Tsyganenko-96. The result shows systematic deviation, and the two conjugate points have a longitude difference about 10 degrees (about 300 km, Figure 8).

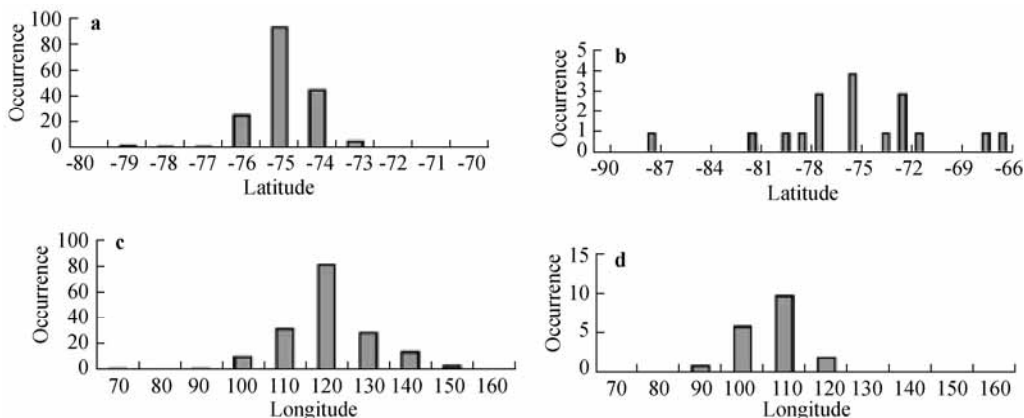


Figure 8 The latitude and longitude (CGM) of LYRC derived from Pc5 cross phase on D and H components, using DAV, ZHS, MAW, and LYR data (b and d), and from Tsyganenko model (a and c).

Huang et al.^[84] compared geomagnetic data of seven auroral substorm events from 15 geomagnetic stations, including Zhongshan Station in Antarctica, Tromsø-Svalbard and East Greenland stations. They discovered that the conjugate point of Zhongshan Station was scattered in a range between Svalbard and East Greenland (Figure 9).

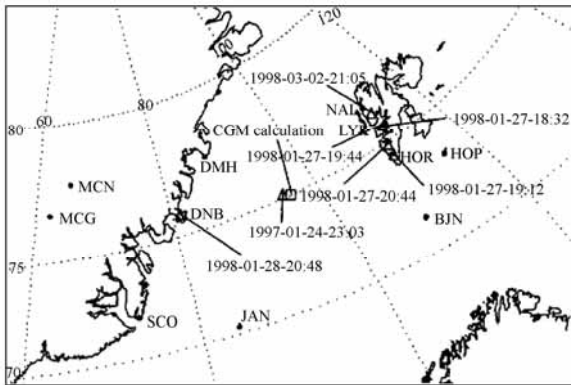


Figure 9 Geomagnetic conjugate points of Zhongshan Station for different geomagnetic events.

Hu et al.^[85] obtained correlation of geomagnetic activity in northern and southern polar regions using geomagnetic data from Zhongshan Station and five other stations in the Arctic, from September 2000 to March 2003 (719 d). Their results show this correlation to be closely related with station location, season, local time and geomagnetic activity. Among the five Arctic stations, Longyearbyen (LYR) had the greatest correlated time with Zhongshan Station (about 17%).

Based on global geomagnetic data in IGY/IGC, Xu^[86] calculated the current systems representing solar and lunar daily variations (S and L) of the geomagnetic field. He compared the south and north polar current systems, and summarized their characteristics as follows: (1) There is remarkable difference in exogenous current systems between the two polar regions. Geomagnetic structure in these regions is the prime reason for this difference. (2) The difference has contributions from a difference in exogenous induced electric field (current) and from a conductivity difference.

Zhu et al.^[87] compared digisonde data from Zhongshan Station with those from Tromsø in the Arctic. Results showed that the peak f_0F2 daily variation was around magnetic noon at Zhongshan Station, but near local noon for Tromsø. Although the geographic latitudes of these sites are similar, their geomagnetic latitudes are not. This means that dayside ionospheres at the two stations are different, being affected by polar convection and dayside photo ionization. Moreover, daily variation of f_0F2 at Zhongshan Station is also affected by ionization produced by auroral precipitating particles in a low solar activity year.

2.7 Space weather in polar regions

Using ground-based instruments at Zhongshan Station, we obtained for the first time systematic datasets of multiple

observations, including of the polar ionosphere, aurora, geomagnetic pulsation and others, during severe solar events. The Antarctic datasets complemented and enriched global observations during the solar maximum years of the 23rd solar cycle. The Zhongshan Station ground-based observations are shown in Figure 10 for the extremely large X-ray solar flare event of 14 July 2004 (the Bastille Day event).

Liu et al.^[88-89], Hu et al.^[90-91] and He et al.^[92] analyzed multiple observation datasets for severe events during solar maximum years of the 23rd solar cycle. They indicated some common behaviors in the response of the polar ionosphere to severe solar events: (a) During the oversized X-ray solar flare event, there were serious polar cap absorptions, with peak value sometimes reaching 26 Db. (b) The first response of the polar ionosphere to catastrophic solar activity is a rapid increase of its F -layer altitude in the initial phase of magnetic storms (this altitude can increase to 200 km), and the frequency of the F layer decreases. During magnetic storms, the ionospheric altitude is disturbed, and the disturbed range exceeds 200 km. Moreover, ionospheric absorption is severe, and the digisonde barely detects the echo because of the absorption. (c) During catastrophic solar activity events, magnetospheric disturbance is also severe. This includes continual, acute magnetospheric and auroral substorms and intense Pc3 and Pc5 geomagnetic pulses in polar regions, which often appear at midday and midnight and at various stages of magnetic storms (not only in the magnetic storm recovery phase). (d) A quantitative statistical relationship was attained, between the sudden absorption of cosmic noise and the X-ray peak flux during flare bursts. Liu et al.^[93] studied ionospheric response of the sub-auroral zone to a geomagnetic storm on 13 March 1983, using ionospheric and geomagnetic data from the Antarctic Great Wall Station.

Xu et al.^[94] proposed a “key-points model” for the current structure and intensity of the polar ionosphere. This summarized six “key points” based on elementary characteristics of the complicated polar current system. This model can be used for space weather.

Using multiple synchronous satellite observations, Han et al.^[95-96] found that the sudden increase of solar wind dynamic pressure can result in earthward injection of protons from the dawn side of the inner magnetosphere. This is a new phenomenon of magnetospheric particle injection that contrasts with particle injection produced by substorms. Liu et al.^[97] investigated the electrodynamics of spontaneous and trigger-associated substorms. Their results show that two typical substorms are very similar. However, spontaneous substorms appear to have a more clearly identifiable growth phase, whereas trigger-associated substorms have a more powerful unloading process.

2.8 Incoherent scatter spectra and ionospheric heating experiments

Wu et al.^[98-101] observed for the first time the polar wind at

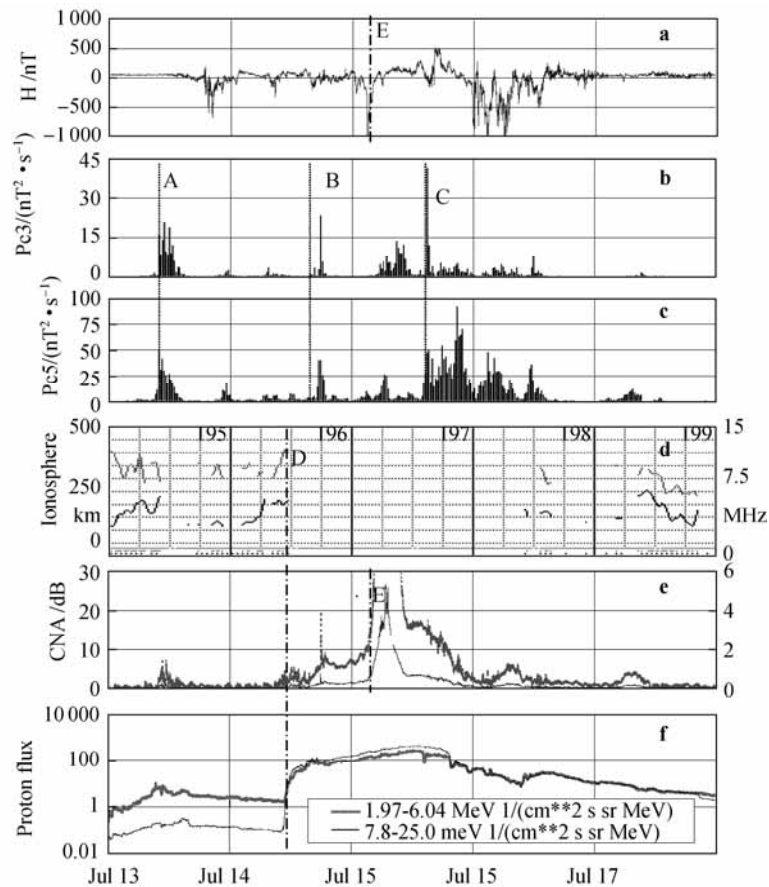


Figure 10 Ground-based observations at Zhongshan Station in Antarctica, and energetic proton flux observation of the SOHO satellite, 13–17 July 2000. **a**, Geomagnetic field H-component. **b**, Pc3 pulsation spectral power. **c**, Pc5 pulsation spectral power. **d**, Ionospheric parameters; lower curve is f_0F_2 , upper curve h_mF_2 . **e**, Riometer absorption at 38.2 MHz; scale of ordinate is 10 dB for lower curve, 2 dB for upper curve. **f**, Proton flux observed by SOHO.

the polar topside ionosphere using EISCAT VHF radar. Zheng and Wu^[102] computed incoherent radar spectra for non-Maxwellian plasma in the high-latitude ionosphere, using a corrected double Maxwellian distribution function to fit the non-Maxwellian distribution, with help from the least square fitting method. Results show that such a corrected double Maxwellian distribution function can simplify calculation of incoherent radar spectra of non-Maxwellian plasma. Xue et al.^[103] and Xu et al.^[104] used a 13-moment approximation of the relaxation model to calculate the distribution function in line-of-sight direction and the incoherent scatter spectra. Xue et al.^[105-106] used the Maxwell molecule collision model to describe ion-neutral collisions of the Boltzmann equation. Viscous and heat flow are included in transport equations, based on the two-Maxwellian distribution. The ion velocity distribution of the Maxwell molecule collision model can be obtained using the 16-moment approximation. According to Grad's theory, Xue et al.^[107] found that the ion velocity distribution function was expanded about a 20-moment approximation based on Maxwellian distribution. They discussed effects of the stress tensor and heat flow vector on the ion velocity distributions. According to Sheffield's theory and the

20-moment approximation, a normalized spectrum is calculated. Finally, the incoherent scatter spectra calculated by the 13-moment approximation and 20-moment approximation are compared (Figure 11). Xu et al.^[108] indicated the incoherent scattering spectrum of collisional plasma with an arbitrary velocity distribution function. Two integrals with complex singular points were solved to obtain the results. The incoherent scatter spectrum during HF heating in the low ionosphere region was computed. The effects of collision frequency, the non-Maxwellian index, electron density, electron temperature and ion temperature on power spectrum were addressed.

Wu et al.^[109] studied the Ohm (heating) effect of high-power radio waves on the Arctic lower ionosphere. They showed that the external pump can modify the temperature of ionospheric plasma, and leads to electron temperature increase, greater collision frequency, and decreased electron loss rates. This in turn modifies electron density. The modification of electron temperature and density decreases with heating time; that is, it tends to be saturated. Using a super-Gaussian electron distribution function, Xue et al.^[110] inverted an incoherent scatter power spectrum recorded during a Chinese campaign with the EISCAT

heating facility. It was concluded that the non-Maxwellian factor should be considered in inversion of incoherent scatter power during ionosphere heating. Xu et al.^[111] examined heating effects in polar winter ionospheric modification experiments of January 2008 at Tromsø, Norway. Results showed a clear disturbance effect under O-mode overdense heating conditions.

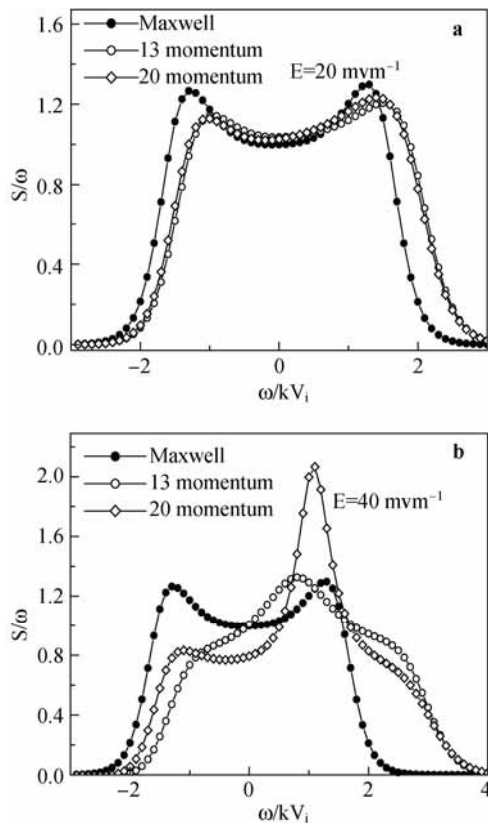


Figure 11 Incoherent scattering spectra in $E \times B$ direction, calculated with Maxwellian distribution, 13 momentum and 20 momentum approximations.

2.9 Studies of polar mesospheric summer echoes

Polar mesospheric summer echoes (PMSE) are anomalous radar echoes, which are found during local summer at mid altitudes (80–90 km) of polar regions. Analyzing ionospheric E and E_s layer irregular characteristics, Li et al.^[112–115] confirmed that PMSE- E_s can be identified at MF and HF bands in the Southern Hemisphere, and roughly explained discrepancies in diurnal and semidiurnal variations using the distribution of the aurora oval. They discovered that the backscattering cross section per unit volume was inversely proportional to the fourth power of the frequency; this relationship differs from that of traditional turbulence theory. There is a mass of charged dust particles in the mesopause, and the differential scattering cross section was used to explain strong echoes with the theory of dusty plasma. The theory of wave propagation in layered media was used to describe PMSE formation.

Shi et al.^[116–118] studied the effect of dust particle

charge and discharge processes on conductivity of dust plasma, and deduced formulation of conductivity and dielectric susceptibility for the dust plasma at weak ionization. They also quantitatively estimated and analyzed characteristic parameters of dust plasma in a rocket exhaust plume and the Earth's polar mesosphere.

2.10 Simulations on polar ionosphere-magnetosphere

Zhu et al.^[119–120] investigated the effect of soft electron precipitation on the polar ionosphere at Zhongshan Station. They also examined summer diurnal variations of f_oF2 and h_m at Great Wall Station, and discussed the effect of neutral wind and upper boundary conditions on f_oF2 and h_m using a one-dimensional and time-dependent theoretical model.

Zhang et al.^[121] performed a simulation to investigate the effects of precipitation electrons on the polar ionosphere. Observation data of precipitating electrons were used as input to the ionospheric model. The f_oF2 resulting from the model correlated very well with observation (Figure 12). Based on statistical characteristics of the ionosphere at Zhongshan Station and the distribution of precipitating electrons in the cusp region, they concluded that the so-called magnetic noon effect at Zhongshan Station is mainly caused by electron precipitation.

Chen et al.^[122] researched the effects of particle precipitation on F -layer electron density in the cusp region, using a one-dimensional and time-dependent ionospheric model. Liu et al.^[123] revealed that the upper boundary condition can greatly influence ionospheric parameters above 200 km. Altitude profiles of temperature are very different from each other, corresponding to O^+ with different upward ion velocities.

Cai et al.^[124] achieved the number density of precipitation electrons, which changes with altitude, energy, and pitch-angle. They did so by numerically solving the transport equation of precipitation electrons, based on the Boltzmann equation. With assumption of a single atmospheric component (N_2), model results gave a good picture of transport rules and characters of the flux spectrum of precipitation electrons in the upper atmosphere of the polar region.

Zhang et al.^[125] studied the response of ionospheric temperature to upward and downward field-aligned current. They showed that expansion/contraction effects are important in electron temperature changes, and can explain the observations well. However, this effect was thought to be secondary. Zhang et al.^[126] simulated conductivity in the electrojet region, indicating that this conductivity could also be affected by the electrojet driven by a strong electric field, and by both external and internal factors. The contribution from internal factors was significant, which makes coupling between magnetosphere and ionosphere more complicated.

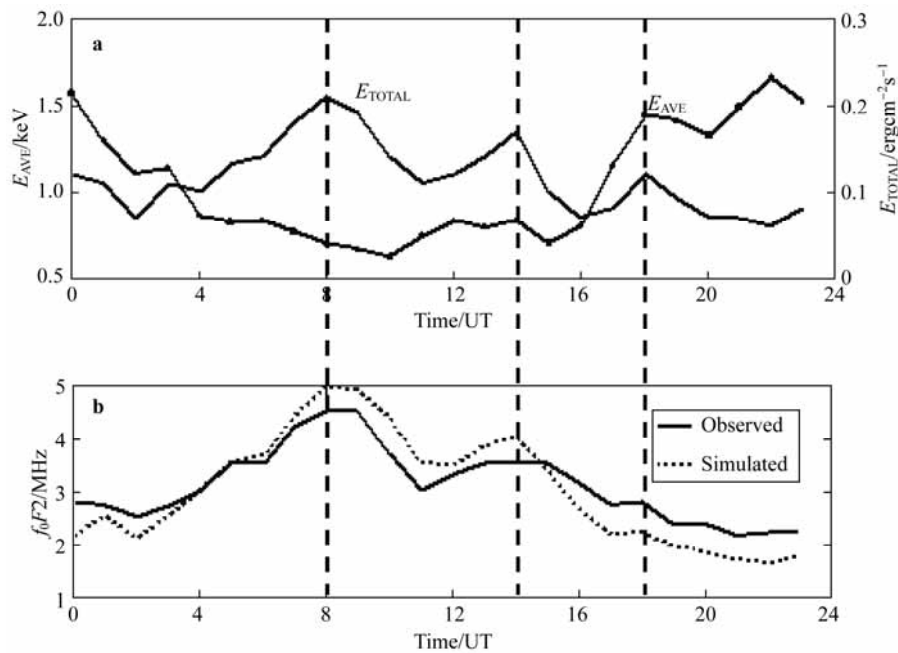


Figure 12 a, Diurnal variation of average energy and total precipitating electron flux at latitudes of cleft. b, Comparison between observed and simulated daily variation of ionospheric f_0F_2 .

3 Summary and prospects

The Chinese Antarctic Great Wall, Zhongshan and Kunlun stations, and Arctic Yellow River Station, have unique geographical locations. They are well suited to make polar upper atmospheric observations. Vigorous development by Chinese Antarctic and Arctic expeditions has created a new research field of polar upper atmospheric physics. Looking back on the active history of nearly 30 years of Chinese polar expeditions, we have achieved remarkable progress in polar upper atmospheric physics research. Highlights of this progress are as follows. An advanced conjugate observation system of polar upper atmospheric physics has been built at the Antarctic Zhongshan Station and Arctic Yellow River Station, which is composed of aurora, ionospheric and geomagnetic instrumentation. Systematic data of more than one solar cycle have been accumulated. Ionospheric variability at cusp region latitudes has been studied and the magnetic noon anomaly has been discovered in the ionospheric F_2 region at Zhongshan Station. The plasma drift pattern at cusp latitudes has been shown for the first time, using ionospheric vertical sounding measurements. The control of IMF B_y on ionospheric drifts has been demonstrated. Synoptic distributions of the post-noon aurora at Zhongshan Station and the dayside aurora at Arctic Yellow River Station have been synthesized, confirming existence of the “15 MLT hot spot” that was first seen in satellite observations. The method of Natural Orthogonal Components (MNOC) has been adopted to study the current system in polar regions, and a “key-point model” proposed for representing this structure in the polar ionosphere. Local time distributions of amplitude and occurrence, and propagation characteristics of Pc3/5 pulsations at cusp latitudes have

been obtained. A method for calculating geomagnetic conjugate location has been proposed based on VLF observations. It has been suggested that solar wind perturbations may directly drive ULF waves in the magnetosphere. The ionospheric signature of high latitude reconnections has been observed. The evolution of flux transfer events (FTEs) generated by dayside reconnections and effects in the polar ionosphere of both hemispheres have been studied. Some regular behaviors in the response of the polar ionosphere to severe solar events have been revealed. Methods have been proposed for calculating incoherent scattering radar spectra for high-latitude ionospheric plasma with a non-Maxwellian distribution. Both the theories of dusty plasma and wave propagation in layered media have been enlisted to explain formation of polar mesospheric summer echoes (PMSE). A three-dimensional and time-dependent model has been developed for simulating the polar ionosphere, which explains well the so-called “magnetic noon anomaly” phenomenon at Zhongshan Station.

Geospace is a significant part of the environment for the survival and development of mankind. Solar storm-induced space weather seriously affects human activity. This brings opportunities and challenges to space weather monitoring, modeling and forecasting. Foreseeing the prospects of polar upper atmospheric research, it should be pointed out that:

(1) The research trend is to treat the upper polar atmosphere as part of geospace, and to study processes systematically and quantitatively. Geospace physics combined with solar physics is entering a new development stage, which emphasizes global behavior of the sun-earth system. It is necessary to study solar wind-magnetosphere-ionosphere coupling and aurora dynamics, including magneto-

sphere-ionosphere dynamic processes dealing with particle precipitation, field currents, convection fields, plasma waves, aurora characteristics and their relation to solar wind-magnetosphere interaction. It is essential to examine polar ionosphere coupling to the neutral atmosphere. This includes the polar ionosphere and its relation to solar activities, polar plasma convection and precipitation, its coupling with the middle and low atmosphere, sudden stratospheric warming events and its relation to the lower ionosphere, the impact of the energetic particle precipitation on the climate system of the Earth, and so on.

(2) Taking advantage of the unique geographic locations of the Chinese polar stations, it is indispensable to investigate inter-hemispheric comparisons in the space environment. This can be done by multi-instrument observations at these geomagnetic conjugate stations. In the future, research will be directed toward very high latitudes of the aurora, cusp and polar cup regions. It is possible to achieve breakthroughs in topics of energy transport and particle precipitation, solar wind control of the polar cup, transition phenomena in the magnetosheath, mechanisms of substorms, and others.

(3) It is mandatory to strengthen basic applied research on space weather. Studies are needed of severe space weather events and their relation to solar conditions, as well as polar ionospheric response to magnetic storms and substorms. It is also critical to study possible ways in which solar energy enters the polar upper atmosphere and how polar ionospheric disturbances propagate towards middle and low latitudes. It is also necessary to explore models and methods for space weather prediction, such as to develop ionospheric physical models in the polar regions. This includes construction of global empirical models by synthesizing multi-measurement data and using assimilation techniques, study of parameters and index systems capable of describing space weather in polar regions, and seeking new directions in space weather nowcasting and forecasting.

(4) Combining ground-based and satellite-borne instruments would be the most important direction for sounding the polar upper atmosphere. It is necessary to improve and upgrade the existing conjugate measurement system, while developing satellite sounding and inversion methods and conducting satellite remote sensing of the aurora and other parameters.

Acknowledgement The authors thank all members of prior Chinese Antarctic and Arctic Scientific Expedition teams. Prof. Xu Wenyao, Prof. Wu Jian and Prof. Zhen Weimin provided relevant materials, and Dr. Hu Zejun assisted in collecting and compiling these.

References

- 1 Wu H, Qian Z H. China Today: China's Antarctic Research Undertakings in Modern Times. Beijing: Contemporary China Publishing House, 1994: 1-548 (in Chinese).
- 2 Liu R Y. Advances in China in the study of solar-terrestrial physics in Antarctica// Xu W Y. Geomagnetism, Atmosphere, Space Research and Applications. Beijing: Seismological Press, 1996: 125-136 (in Chinese).
- 3 Liu R Y, Yang H G, Qian S L, et al. The Upper Atmosphere Comprehensive Observations System and its application at Zhongshan Station, Antarctica// Chen L X. The Research of Antarctica's response and feedback to Global Change. Beijing: Ocean press, 2004: 249-258 (in Chinese).
- 4 Lu D R, Fu Q J, Xu W Y, et al. The comprehensive observations and study of solar-terrestrial's overall behavior in Antarctica // Chinese Arctic and Antarctic Administration. Chinese Antarctica Scientific Research and Progress. Beijing: Ocean Press, 1998: 537-543.
- 5 Cao C, Wang S L, Xi D L. Analysis of the ionospheric data from 1986 to 1988 obtained at the Great Wall Station of China, Antarctic. Chinese Journal of Radio Science, 1992, 7(2): 39-46 (in Chinese).
- 6 Cao C. A comparison of ionospheric characteristic at two stations with similar geomagnetic latitudes. Chinese Journal of Radio Science, 1993, 8(2): 84-91 (in Chinese).
- 7 Zeng W M, Cao C, Wu J. Analysis of the ionospheric anomaly over Great Wall Station, Antarctica. Antarctic Research, 1994, 6(3): 33-37 (in Chinese).
- 8 Zhen W M, Cao C, Wu J, et al. Investigations on relationship between ionospheric disturbance and neutral winds during geomagnetic storms at the Great Wall Station, Antarctic. Chinese Journal of Radio Science, 1995, 10(3): 76-79 (in Chinese).
- 9 Liu R Y, Qian S L, He L S. Preliminary experimental results about the digisonde portable sounder-4 at Zhongshan station, Antarctica. Chinese Journal of Geophysics, 1997, 12(4): 109-118 (in Chinese).
- 10 Liu S L, He L S, Liu R Y. Mean ionospheric properties in winter at Zhongshan Station, Antarctica. Chinese Journal of Polar Research, 1997, 9(3):192-197 (in Chinese).
- 11 Shen C S, Zi M Y, Wang J S, et al. The features of f_oF_2 at Zhongshan station of Antarctica. Chinese Journal of Polar Research, 2003, 15(3): 186-194 (in Chinese).
- 12 He L S, Liu Y H, Liu R Y. The average feature of ionosphere in solar minimum at Zhongshan Station. Chinese Yearbook of Geophysics, 1998.
- 13 He L S, Liu R Y, Liu S L, et al. Overall properties of F region around solar minimum at Zhongshan Station, Antarctica. Chinese Journal of Geophysics, 2000, 43(3): 289-295 (in Chinese).
- 14 Shen C S, Zi M Y, Wang J S, et al. Features of the polar ionosphere over the Zhongshan Station in Antarctic. Chinese Journal of Geophysics, 2005, 48(1): 1-6 (in Chinese).
- 15 Liu S L, Liu R Y, He L S. The high-latitude ionospheric phenomena observed by DPS-4 at Zhongshan Station, Antarctica. Chinese Journal of Polar Science, 1999, 10(2): 141-148.
- 16 Xu Z H, Liu R Y, Liu S L. Variations of the ionospheric F_2 layer critical frequency at Zhongshan Station, Antarctica. Chinese Journal of Geophysics, 2006, 49(1): 1-8 (in Chinese).
- 17 He L S, Liu R Y, Liu S L, et al. Seasonal characteristics of F region in lower solar activity period at Zhongshan Station, Antarctica. Chinese Journal of Polar Science, 1999, 10(2): 149-154.
- 18 Alfonis L, Kavanagh A J, Amata E, et al. Probing the high latitude ionosphere from ground-based observations: The state of current knowledge and capabilities during IPY (2007-2009). Journal of Atmospheric and Solar-Terrestrial Physics, 2009, 70(18): 2293-2308.
- 19 Liu R Y, He L S, Hu H Q, et al. Ionospheric absorption at Zhongshan Station, Antarctica during magnetic storms in early May, 1998. Chinese Journal of Polar Science, 1999, 10(2): 133-140.
- 20 Nishino M, Yamagishi H, Sato N, et al. Initial results of imaging riometer observations at Polar Cap Conjugate Stations, Proc. NIPR. Upper Atmospheric Physics, 1998, 12: 58-72.
- 21 Nishino M, Yamagishi H, Sato N, et al. Post-noon ionospheric absorption observed by the imaging riometers at polar cusp/cap conjugate stations. Chinese Journal of Polar Science, 1999, 10(2): 125-132.
- 22 Nishino M, Yamagishi H, Sato N, et al. Conjugate features of dayside

- absorption associated with specific changes in the solar wind observed by inter-hemispheric high-latitude imaging riometers. *Advances on Polar Upper Atmosphere Research*, 2000, 14:76-92.
- 23 Yamagishi H, Fujita Y, Sato N, et al. Interhemispheric conjugacy of auroral poleward expansion observed by conjugate imaging riometers at $\sim 67^\circ$ and $75^\circ - 77^\circ$ invariant latitude. *Advances on Polar Upper Atmosphere Research*, 2000, 14: 12-33.
 - 24 Deng Z X, Liu R Y, Zhao Z Y, et al. Polar ionospheric absorptions during solar storms at the end of October, 2003. *Chinese Journal of Polar Research*, 2005, 17(1): 23-31 (in Chinese).
 - 25 Deng Z X, Liu R Y, Zhao Z Y, et al. Statistical characteristics of ionospheric absorption spike events at Zhongshan Station. *Chinese Journal of Space Science*, 2006, 3: 172-176 (in Chinese).
 - 26 Wan W X, Liu L B, Parkinson M L, et al. The effect of fluctuating ionospheric electric fields on Es-occurrence at cusp and polar cap latitudes. *Advances in Space Research*, 2001, 27(6-7): 1283-1288.
 - 27 Meng Y, Wang Z M, E D C, et al. Research of Polar TEC fluctuations and polar patches during magnetic storm using GPS. *Chinese Journal of Geophysics*, 51(1): 17-24 (in Chinese).
 - 28 Cai H T, Ma S Y, Schlegel K. Climatologic characteristics of high-latitude ionosphere- EISCAT observations and comparison with the IRI model. *Chinese Journal of Geophysics*, 2005, 48(3): 471-479 (in Chinese).
 - 29 Liu Y C, Ma S Y, Cai H T, et al. The background ionospheric profiles at polar cusp latitudes - ESR observations. *Chinese Journal of Polar Research*, 2005, 17(3): 193-202 (in Chinese).
 - 30 Zhang Q H, Zhang B C, Liu R Y, et al. On the importance of interplanetary magnetic field $|B_y|$ on polar cap patch formation. *Journal of Geophysical Research*, 2011, 116(A05308), doi:10.1029/2010JA016287.
 - 31 Zhou G C, Wang D J. Electrostatic Ion Cyclotron and Ion Acoustic Wave Instabilities Driven by Upgoing Oxygen Ion (O^+) Beams on Auroral Field Lines. *Chinese Journal of Space Science*, 1987, 7(2): 103-116 (in Chinese).
 - 32 Song L T, Wang X W. Alfvén travelling surge with parallel electric field-auroral particle acceleration mechanism. *Chinese Journal of Geophysics*, 1995, 38(1): 6-15 (in Chinese).
 - 33 Song L T. A two-dimensional model of the westward traveling surge. *Chinese Journal of Space Science*, 1989, 9(1): 13-19 (in Chinese).
 - 34 Tai H S. The Ratio of $OI\ 5557$ to $N^{2+}\ 3914$ under Diffuse Auroral Condition. *Chinese Journal of Space Science*, 1985, 5(1): 34-39 (in Chinese).
 - 35 Cao C. The diurnal variation of the occurrence of pulsating Aurora over DAVIS. *Chinese Journal of Radio Science*, 1986, 1(4): 7-14.
 - 36 Xi D L. The diurnal and seasonal variations of the auroral absorptions. *Antarctic Research*, 1988, 1(2): 54-58 (in Chinese).
 - 37 Jorma K, Cao C. Pulsating aurora—a review. *Antarctic Research*, 1995, 6(1): 39-50.
 - 38 Hu H Q, Liu R Y, Wang J F, et al. Statistic characteristics of the auroral observed at Zhongshan Station, Antarctica. *Chinese Journal of Polar Research*, 1999, 11(1): 8-18 (in Chinese).
 - 39 Yang H G, Liu R Y, Huang D H, et al. An all-sky auroral video image analyzing system. *Chinese Journal of Geophysics*, 1997, 40(5): 606-615 (in Chinese).
 - 40 Yang H G, Liu R Y, Sato N. Intensity correction in all-sky auroral image projection transforms. *Chinese Science Bulletin*, 1997, 42(8): 37-40.
 - 41 Yang H, Sato N, Makita K, et al. Synoptic observations of auroras along the postnoon oval: A survey with all-sky TV observations at Zhongshan, Antarctica. *Journal of Atmospheric and Solar-Terrestrial Physics*, 2000, 62: 787-797.
 - 42 Hu Z J, Yang H G, Ai Y, et al. Multiple wavelengths observations of day-side auroras in visible range-A preliminary result of the first wintering auroral observations in Chinese Arctic Station at Ny-Ålesund. *Chinese Journal of Polar Research*, 2005, 17(2): 107-114 (in Chinese).
 - 43 Hu Z J, Yang H G, Huang D H, et al. Synoptic distribution of dayside aurora: Multiple-wavelength all-sky observation at Yellow River Station in Ny-Ålesund, Svalbard. *Journal of Atmospheric and Solar-Terrestrial Physics*, 2009, 71(6): 794-804.
 - 44 Wang Q, Liang J, Hu Z J, et al. Spatial texture based automatic classification of dayside aurora in all-sky images. *Journal of Atmospheric and Solar-Terrestrial Physics*, 2010, 72: 498-508.
 - 45 Hu Z J, Yang H G, Liang J, et al. The 4-emission-core structure of dayside aurora oval observed by all-sky imager at 557.7 nm in Ny-Ålesund, Svalbard. *Journal of Atmospheric and Solar-Terrestrial Physics*, 2010, 72: 638-642.
 - 46 Zhang Q H, Dunlop M W, Lockwood M, et al. Simultaneous observations of reconnection pulses at Cluster and their effects on the cusp aurora observed at the Chinese Yellow River Station. *Journal of Geophysical Research*, 2010, 115(A10237), doi:10.1029/2010JA015526.
 - 47 Yang Y H, Tang K Y, Liu R Y, et al. Analyzing of the aurora and geomagnetic disturbance in Zhongshan station, Antarctica. *Chinese Journal of Polar Research*, 1999, 11(3): 228-234 (in Chinese).
 - 48 Hu H Q, Liu R Y, Wang J F, et al. Postnoon aurora observed at Zhongshan Station, Antarctica during magnetic disturbance—A case Study. *Chinese Journal of Radio Science*, 1999, 14(s): 31-34 (in Chinese).
 - 49 Hu H Q, Liu R Y, Yang H G, et al. Postnoon aurora observed at Zhongshan Station, Antarctica during quiet period—A case Study. *Journal of Wuhan University (Natural Science Edition)*, 1999, 45(5A): 639-642 (in Chinese).
 - 50 Hu H Q, Liu R Y, Yang H G, et al. Dependence of the postnoon auroral intensity upon the solar wind parameters. *Chinese Journal of Polar Research*, 2001, 13(3): 151-158 (in Chinese).
 - 51 Hu H Q, Liu R Y, Yang H G, et al. Dependence of the postnoon auroral intensity upon the IMF. *Chinese Journal of Geophysics*, 2002, 45(4): 445-452 (in Chinese).
 - 52 Hu H Q, Liu R Y, Yang H G. Dependences of postnoon auroral intensity on solar wind-magnetosphere coupling functions. *Chinese Journal of Space Science*, 2006, 26(4): 241-249 (in Chinese).
 - 53 Hong M H, Hu H Q, Liu R Y, et al. Nightside auroral arcs in high latitudes during substorms and their relationship with IMF. *Chinese Journal of Geophysics*, 2001, 44(1): 12-23 (in Chinese).
 - 54 Hong M H, Wang X M, Chua D, et al. Auroral substorm response to solar wind pressure shock. *Chinese Science Bulletin*, 2001, 46(18): 1547-1551.
 - 55 Sato N, Murata Y, Yamagishi H, et al. Simultaneous observations of Syowa East HF radar and Zhongshan Station optical aurora associated with the solar wind negative pressure impulse. *Chinese Journal of Polar Science*, 1999, 10(2): 81-88.
 - 56 Sato N, Murata Y, Yamagishi H, et al. Enhancement of optical aurora triggered by the solar wind negative pressure impulse (SI-). *Geophysics Research Letter*, 2001, 28(1): 127-130.
 - 57 Liu J J, Hu H Q, Han D S, et al. Decrease of auroral intensity associated with reversal of plasma convection in response to an interplanetary shock as observed over Zhongshan in Antarctica. *Journal of Geophysical Research*, 2010, 116(A03210), doi:10.1029/2010JA016156.
 - 58 Cai H T, Ma S Y. Initial study of inversion method for estimating energy spectra of auroral precipitating particle from ground-based IS radar observations. *Chinese Journal of Geophysics*, 2007, 50(1): 10-17 (in Chinese).
 - 59 Liu J M, Zhang B C, Liu R Y, et al. Effects of the precipitation electrons on the polar ionosphere with different energy spectrum. *Chinese Journal of Geophysics*, 2009, 52(6): 1429-1437 (in Chinese).
 - 60 Chen H F, Xu W Y. Variations of inner magnetospheric currents during the magnetic storm of May 1998. *Chinese Journal of Geophysics*, 2001, 44(4): 490-499 (in Chinese).
 - 61 Shen C S, Zi M J, Gao Y F, et al. Geomagnetic responses to the convection field, field-aligned current and auroral electrojet. *Chinese Journal of Geophysics*, 1999, 42(6): 725-731 (in Chinese).

- 62 Xu W Y. Eigen mode analysis of the equivalent ionospheric current system in the polar region during substorms. *Progress in Geophysics*, 1999, 14(Supplement): 36-42 (in Chinese).
- 63 Xu W Y, Sun W. A study on the multi-component substorm current. *Chinese Journal of Polar Science*, 2000, 11:53-58.
- 64 Sun W, Xu W Y, Akasofu S I. An improved method to deduce the unloading component for magnetospheric substorms. *Journal of Geophysics Research*, 2000, 105(A6): 13131-13140.
- 65 Xu W Y, Chen G X. Quantitative analysis of the relationship between polar ionospheric currents and auroral electrojet indices. *Science in China(Series D)*, 2005, 48(3): 376-383.
- 66 Xu W Y. Variations of the auroral electrojet belt during substorms. *Chinese Journal of Geophysics*, 2009, 52(3): 607-615 (in Chinese).
- 67 Liu R Y, Zhu Y Q. Ionospheric drift properties and its response to the IMF conditions at Zhongshan station, Antarctica. *Chinese Journal of Geophysics*, 1999, 42(1): 30-40 (in Chinese).
- 68 Zhang Q H, Liu R Y, Huang J Y, et al. Characteristics of the magnetic flux transfer events on April 1 of 2004. *Chinese Journal of Polar Research*, 19(2): 121-130.
- 69 Zhang Q H, Liu R Y, Huang J Y, et al. Simultaneous Cluster and Cutlass observations of FTEs on 11 February 2004. *Chinese Journal of Geophysics*, 2008, 51(1): 1-9.
- 70 Zhang Q H, Liu R Y, Dunlop M W, et al. Simultaneous tracking of reconnected flux tubes: Cluster and conjugate SuperDARN observations on 1 April 2004. *Annales Geophysicae*, 2008, 26: 1545-1557.
- 71 Hu H, Yeoman T K, Lester M, et al. Dayside flow bursts and high latitude reconnection when the IMF is strongly northward. *Annales Geophysicae*, 2006, 24: 2227-2242.
- 72 Yang S F, Xiao F H. The characteristics of Pc3 pulsations at Great Wall station of Antarctica. *Antarctic Research*, 1994, 6(2): 62-67 (in Chinese).
- 73 Yang S F, Du A M, Chen B S. The characteristics of Pc3 pulsations at Zhongshan station of Antarctica. *Chinese Journal of Geophysics*, 1997, 40(3): 311-316 (in Chinese).
- 74 Yang S F, Du A M, Chen B S. Observation and analyses of geomagnetic pulsations at Zhongshan station, Antarctica. *Chinese Journal of Polar Research*, 1997, 9(1): 58-65 (in Chinese).
- 75 Liu Y H, Liu R Y, Yang S F, et al. Propagation characteristics of the Pc3 frequency range pulsation in the cusp latitudes. *Chinese Journal of Polar Research*, 2000, 12(2): 121-128 (in Chinese).
- 76 Liu Y H, Liu R Y, Yang S F, et al. Propagation and origin of Pc5 frequency range pulsation in the cusp latitude. *Chinese Journal of Geophysics*, 2001, 44(z1): 8-15 (in Chinese).
- 77 Liu Y H, Liu R Y, Yang S F, et al. A study of the Pc3 pulsation in the cusp latitudes by short based-line. *Chinese Journal of Geophysics*, 2001, 44(z1): 16-21 (in Chinese).
- 78 Liu Y H, Liu R Y, Hu H Q, et al. Study and observation of the great solar event in July of 2000 at cusp latitude. *Chinese Journal of Polar Research*, 2001, 13(3): 205-212 (in Chinese).
- 79 Yang S F, Liu Y H. Polarization characteristics of pc3 pulsations at Zhongshan Station of Antarctica. *Chinese Journal of Polar Science*, 1999, 10(2): 155-163.
- 80 Han D S, Yang H G, Chen Z T, et al. Coupling of perturbations in the solar wind density to global Pi3 pulsations: A case study. *Journal of Geophysics Research*, 2007, 112(A05217), doi:10.1029/2006JA011675.
- 81 Liu Y H, Fraser B J, Ables S T, et al. Transverse-scale size of Pc3 ULF waves near the exterior cusp. *Journal of Geophysics Research*, 2009, 114(A08208), doi:10.1029/2008JA013971.
- 82 Shi R, Zhao Z Y, Zhang B C. Study of the influence of IAR on geomagnetic signal observed on the ground. *Chinese Journal of Geophysics*, 2010, 53(5): 693-703.
- 83 Liu Y H, Fraser B J, Liu R Y, et al. Conjugate phase studies of the ULF waves in the Pc5 band near the cusp. *Journal of Geophysics Research*, 2003, 108(A7): 1247, doi:10.1029/2002JA009336.
- 84 Huang D H, Moen J, Brekke A, et al. Zhongshan conjugate point study during auroral substorms. *Chinese Journal of Geophysics*, 2004, 47(1): 54-60 (in Chinese).
- 85 Hu H Q, Liu R Y, Yang H G, et al. Cross correlations of geomagnetic field variations between Zhongshan and Arctic stations. *Chinese Journal of Geophysics*, 2006, 49(5): 1321-1328 (in Chinese).
- 86 Xu W Y. A comparative study on the ionospheric current systems in the Antarctic and Arctic regions. *Antarctic Research*, 1994, 6(1): 8-16 (in Chinese).
- 87 Zhu A Q, Zhang B C, Huang J Y, et al. Comparative study of winter polar ionospheric F2 layer in both hemispheres. *Chinese Journal of Polar Research*, 2008, 20(1): 31-39 (in Chinese).
- 88 Liu R Y, Hu H Q, Liu Y H, et al. Responses of the polar ionosphere to the Bastille Day solar event. *Solar Physics*, 2001, 204(1-2): 307-315.
- 89 Liu R Y, Hu H Q, He L S, et al. Multiple ground-based observations at Zhongshan Station during the April/May 1998 solar events. *Science in China (Series A)*, 2002, 45(9): 120-131.
- 90 Hu H Q, Liu R Y, Liu Y H, et al. The polar ionosphere at Zhongshan Station on May 11, 1999, the day the solar wind almost disappeared. *Science in China (Series A)*, 2002, 45(S1): 161-166.
- 91 Hu H Q, Liu R Y, Liu Y H, et al. The intense ionospheric absorptions associated with R9077. *Chinese Journal of Space Science*, 2002, 22(1): 13-20 (in Chinese).
- 92 He L S, Nishino M, Zhang B C, et al. Absorption events associated with solar flares. *Chinese Science Bulletin*, 2001, 46(5): 369-372.
- 93 Liu R Y, Liu S L, Wen B, et al. Ionospheric effects of the march 13, 1989 magnetic storm at subauroral region. *Antarctic Research (Chinese Edition)*, 1994, 6(1): 17-24.
- 94 Xu W Y, Chen G X, Du A M, et al. Key points model for polar region currents. *Journal of Geophysics Research*, 2008, 113(A3), A03S11, doi:10.1029/2007JA012588.
- 95 Han D S, Yang H G, Nosé M, et al. Dawnside particle injection caused by sudden enhancement of solar wind dynamic pressure. *Journal of Atmospheric and Solar-Terrestrial Physics*, 2008, 70(16): 1995-1999.
- 96 Han D S, Yang H G, Liang J, et al. High-latitude reconnection effect observed at the dayside dip equator as a precursor of a sudden impulse. *Journal of Geophysics Research*, 2010, 115(A08214), doi:10.1029/2009JA014787.
- 97 Liu J M, Zhang B C, Kamide Y, et al. Spontaneous and trigger-associated substorms compared: Electrodynamic parameters in the polar ionosphere. *Journal of Geophysics Research*, 2011, 116(A01207), doi:10.1029/2010JA015773.
- 98 Wu J, Blanc M, Alcayde D. The ionospheric polar wind observations with EISCAT VHF radar. *Chinese Journal of Geophysics*, 1993, 36(1):9-17 (in Chinese).
- 99 Wu J, Blanc M, Alcayde D, et al. Observations of the structure and vertical transport of the polar upper ionosphere with the EISCAT VHF radar. 2. First investigations of the topside O⁺ and H⁺ vertical ion flows. *Annales Geophysicae*, 1992, 10: 375-393.
- 100 Wu J, Tiaeb C. Heat flux solution of the 13-moment approximation transport equations in a multispecies gas. *Journal of Geophysics Research*, 1993, 98(A9): 15613-15619.
- 101 Wu J, Tiaeb C. Heat flux and thermal conduction in O⁺ and H⁺ ion flows deduced from EISCAT-VHF radar observations in the high-latitude topside ionosphere. *Journal of Geophysics Research*, 1994, 99(A6): 11483-11494.
- 102 Zheng C Q, Wu J. A computation of the incoherent radar spectra of non-maxwellian plasma in the high-latitude ionosphere. *Chinese Journal of Geophysics*, 1994, 37(4): 433-439 (in Chinese).
- 103 Xue K, Xu B, Wu J, et al. Relaxation model of incoherent scatter spectra calculation. *Progress in Natural Science*, 2007, 17(11): 1565-1571 (in

- Chinese).
- 104 Xu B, Xue K, Wu J, et al. Incoherent scatter spectra from plasma of a 13-moment approximation distribution function. *Science in China (Series E)*, 2008, 51(5): 624-631.
- 105 Xu K, Guo L X, Wu J, et al. The ion distribution function from Maxwell molecule collision model and calculations of incoherent scatter spectra. *Chinese Journal of Space Science*, 2009, 29(3): 287-295.
- 106 Xue K, Guo L X, Wu J, et al. 16-moment approximation for ion velocity distribution and its application in calculations of incoherent scattering spectra. *Plasma Science and Technology*, 2009, 11(2): 152-158.
- 107 Xue K, Guo L X, Wu J, et al. Application of 20-moment approximation for ion velocity distribution function in calculations of incoherent scatter spectra. *Chinese Journal of Geophysics*, 2009, 52(4): 878-886 (in Chinese).
- 108 Xu B, Wu Z S, W J, et al. Incoherent scatter spectrum of a collisional plasma. *Acta Physica Sinica*, 2009, 58(7): 5104-5110 (in Chinese).
- 109 Wu J, Che H Q, Wu J, et al. A simulation of the heating effect of high power radio wave on the lower polar ionosphere. *Chinese Journal of Polar Research*, 2007, 19(3): 171-180 (in Chinese).
- 110 Xu B, Wu Z S, Wu J, et al. Inversion of incoherent scatter spectra during ionosphere heating. *Chinese Journal of Radio Science*, 2008, 23(4): 713-716 (in Chinese).
- 111 Xu B, Wu J, Wu J, et al. Observations of the heating experiments in the polar winter ionosphere. *Chinese Journal of Geophysics*, 2009, 52(4): 859-877 (in Chinese).
- 112 Li H L, Wu J, Liu R Y, et al. The statistics analysis of mesosphere summer echoes observed by DPS-4 at Zhongshan station, Antarctica. *Chinese Journal of Polar Research*, 2007, 19(1): 1-9 (in Chinese).
- 113 Li H L, Wu J, Huang J Y, et al. Preliminary analysis on the relationship between polar mesosphere summer echoes and frequency. *Chinese Journal of Space Science*, 2007, 27(5): 416-419 (in Chinese).
- 114 Li H L, Wu J, Huang J Y, et al. Scattering of electromagnetic wave by charged dust in polar mesopause. *Chinese Journal of Radio Science*, 2008, 23(4): 686-688 (in Chinese).
- 115 Li H L, Wu J, Zhang Y, et al. Study on relationship between reflecting characteristic of polar mesosphere summer echoes with frequency. *Journal of China Academy of electronics and information Technology*, 2008, 3(5): 474-477 (in Chinese).
- 116 Shi Y X, Ge D B, Wu J. Influence of charge and discharge processes of dust particles on the dust plasma conductivity. *Acta Physica Sinica*, 2006, 55(10): 5318-5323 (in Chinese).
- 117 Shi Y X, Wang J, Wu J, et al. Characteristic parameters estimation of two weakly ionized dusty plasma. *Chinese Journal of Radio Science*, 23(1): 95-99 (in Chinese).
- 118 Shi Y X, Wu J, Ge D B. The research on the dielectric tensor of weakly ionized dust plasma. *Acta Physica Sinica*, 58(8): 5507-5512 (in Chinese).
- 119 Zhu M H, Cao C, Wu J. Numerical Modeling of the Ionospheric Variations over the Great Wall Station, Antarctica. *Chinese Journal of Space Science*, 1997, 17(4): 337-342 (in Chinese).
- 120 Zhu M H, Cao C, Wu J. Analyses of Ionospheric Properties Over Zhongshan Station Antarctica. *Chinese Journal of Radio Science*, 1996, 11(1): 96-101 (in Chinese).
- 121 Zhang B C, Liu R Y, Liu S L. Simulation study on the influences of the precipitating electrons on the polar ionosphere. *Chinese Journal of Geophysics*, 2001, 44(3): 311-319 (in Chinese).
- 122 Chen Z T, Zhang B C, Yang H G, et al. A simulation study on ionosphere affected by auroral particle precipitation in cusp region. *Chinese Journal of Polar Research*, 2006, 18(3): 166-174 (in Chinese).
- 123 Liu S L, Zhang B C, Liu R Y, et al. The influence of upper boundary conditions on the polar ionosphere. *Chinese Journal of Space Science*, 2005, 25(6): 504-509 (in Chinese).
- 124 Cai H T, Ma S Y, Pu Z Y. Numerical study of the auroral particle transport in the polar upper atmosphere. *Science in China (Series E)*, 2008, 51(10): 1759-1771.
- 125 Zhang B C, Kamide Y, Liu R Y. Response of electron temperature to field-aligned current carried by thermal electrons: A model. *Journal of Geophysics Research*, 2003, 108(A5), 1169, doi:10.1029/2002JA009532.
- 126 Zhang B C, Kamide Y, Liu R Y, et al. A modeling study of ionospheric conductivities in the high-latitude electrojet regions. *Journal of Geophysics Research*, 2004, 109(A04310), doi:10.1029/2003JA010181.